Outage Performance of Hybrid Satellite-Aerial-Terrestrial Networks in the Presence of Interference

Anuradha Verma*, Deepika Gupta†, and Pankaj K. Sharma*
*Department of Electronics and Communication Engineering,
National Institute of Technology Rourkela, Odisha, India
†Department of Electronics and Communication Engineering,
Dr. S. P. M. International Institute of Information Technology, Naya Raipur, Chhattisgarh, India
Email: 519ec1026@nitrkl.ac.in, deepika@iiitnr.edu.in, sharmap@nitrkl.ac.in

***Abstract*—In this paper, we consider a hybrid satellite-aerial-terrestrial network (HSATN) where the dual-hop communication from a satellite to ground user equipment (UE) is aided by a static aerial relay in the presence of interference. Specifically, we consider multiple high altitude platforms (HAPs) located in a 3-dimensional spherical sector above the surface of earth as interferers to the aerial relay. Further, we consider a single low altitude platform (LAP) located in a cylindrical terrestrial small cell to which act as an interferer to ground UE. By assuming the shadowed-Rician fading for satellite/HAPs links, the Rician fading for aerial relay link, and Nakagami-*m* fading for LAP link, we derive the outage probability (OP) of first and second hops as well as the end-to-end satellite to ground UE transmissions. Further, we depict the impact of underlying system parameters on the OP of considered HSATN. We verify our analytical results through simulations.**

I. Introduction

Satellite networks have received tremendous interest for global coverage at a significantly low cost. Traditionally, satellite networks have been deployed for facilitating the communication between a satellite and an outdoor ground user equipment (UE) [1], [2]. However, in practice, the communication link between satellite and ground UE gets frequently masked due to adverse atmospheric conditions such as heavy clouds, rain, etc., and suffer from severe fading. Further, in recent times, the application of satellite networks has not been limited to outdoor communications only. In fact, the satellite networks have been considered for enabling internet services for indoor ground UEs in certain applications, e.g., enhanced mobile broadband (eMBB). However, due to the transmit power constraint at satellite causes significant hindrance to achieve reliable satellite-to-ground UE communications in the aforementioned scenarios. To address this issue, the concept of hybrid satellite-terrestrial network (HSTN) has been proposed in literature where the satellite-to-ground UE communication is aided by a terrestrial relay which has strong connectivity with the satellite as well as ground UE [3], [4].

On the other hand, backed by the low-cost and portability feature, the unmanned aerial vehicles (UAVs) have found use in wireless communications as flying base station, wireless access point, mobile relay, etc., to provide coverage in complex terrains (e.g., on hills, sea, marshes, etc.), hotspot scenarios (e.g., during grand social events, etc.), and infrastructure damage (e.g., in natural disasters, etc.) [5]-[7]. Relying on the merits of UAVs, the terrestrial relay in a conventional HSTN has been eventually replaced by a mobile UAV relay to form a hybrid satellite-aerial-terrestrial network (HSATN) which has received a lot of research attention recently [8].

The works in [4], [9]-[11] have investigated the performance of HSTNs with decode-and-forward (DF)/amplify-and-forward (AF) relaying without considering the impact of co-channel interference (CCI). Further, the works in [12]-[14] have analyzed the performance of HSTNs in the presence of CCI from terrestrial interfering sources. In contrast, the work in [15] have investigated the performance of an overlay cognitive HSTN by taking into account the combined interference from terrestrial as well as extra-terrestrial interfering sources. Note that all the aforementioned works were based on the performance analysis of HSTNs with ground-based relays. It is worth mentioning that the UAVs as aerial relays have recently been incorporated into wireless networks owing to their several benefits over the ground relays [16], [17]. Consequently, the HSATNs which utilize the UAVs as relays have been investigated in the works [18]-[20]. However, none of these works have considered the impact of interference on the performance of HSATNs. Since HSATNs have a three-dimensional (3D) network configuration with UAV relays, it is prone to receive interference from co-channel aerial sources such as high altitude platforms (HAPs) and low altitude platforms (LAPs). The most common form of HAPs are balloons deployed for wider coverage on ground as compared to the LAPs which include UAV nodes much closer to ground. Therefore, to analyze the performance of HSATNs by taking into account the interference from both HAP and LAP interferers is currently an open problem.

Motivated by the above, in this paper, we investigate the performance of a dual-hop HSATN where a satellite communicates with a ground UE via a static UAV relay in the presence of interference.

Specifically, we consider multiple HAP interferers located in a 3D spherical sector above the surface of earth causing interference to the aerial relay in the first hop. We further

978-1-6654-2337-3/21/$31.00 © 2021 IEEE

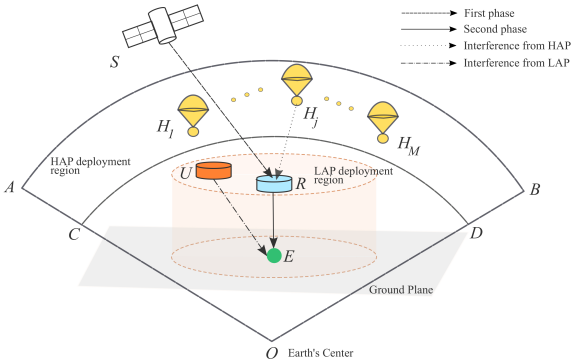

Fig. 1. HSATN system model.

consider a single low altitude platform (LAP) interferer located in a cylindrical terrestrial small cell which causes interference to ground UE in the second hop. Considering the shadowed-Rician fading for satellite/HAPs links, the Rician fading for aerial relay link, and the Nakagami-*m* fading for LAP link, we derive the outage probability (OP) of individual hops' and end-to-end (e2e) transmissions. We draw useful insights on the system performance based on the impact of underlying system parameters.

II. System Description

A. System Model

We consider an HSATN where a geostationary earth orbit (GEO) satellite S sends its message signals to a fixed ground UE E with the assistance of a decode-and-forward (DF) aerial relay R as shown in Fig 1. Herein, we assume that the aerial relay R is located at a fixed altitude of w_{re} vertically above the UE E. We further assume that a group of HAPs H_j, $j \in \{1, ..., M\}$ coexisting in a three-dimensional spherical sectorial region $ABDC$ from the center of earth O cause interference to aerial relay R in the first hop. Likewise, we assume that a LAP U deployed uniformly random at the top of a cylindrical region around E with radius L and height w_{re} cause interference to E in the second hop. The channel coefficients for $S \to R$ and $H_j \to R$ are denoted by g_{sr} and $g_{h_j r}$, respectively, and are subject to shadowed-Rician (SR) fading. Further, the channel coefficients for $R \to E$ and $U \to E$ links are denoted by g_{re} and g_{ue}, respectively. Here, g_{re} and g_{ue} are assumed to follow Rician and Nakagami-*m* fading, respectively. Moreover, the w_{sr}, $w_{h_j r}$, and w_{ue} represent the distances between nodes S and R, H_j and R, and U and E, respectively. All receivers are assumed to be corrupted by the additive white Gaussian noise (AWGN) with mean zero and variance σ^2.

B. Channel Models

1) $S \to R$ and $H_j \to R$ links' channels: The channel g_{ir}, $i \in \{s, h_j\}$ are assumed to follow the independent SR fading . Hence, the probability density function (pdf) of squared channel $|g_{ir}|^2$ is given by [11]

$$f_{|g_{ir}|^2}(x) = \alpha_{ir} \sum_{\kappa=0}^{m_{ir}-1} \zeta(\kappa) x^{\kappa} \mathrm{e}^{-(\beta_{ir}-\delta_{ir})x}, \tag{1}$$

where $\alpha_{ir} = (2\mathrm{b}_{ir} m_{ir}/(2\mathrm{b}_{ir} m_{ir} + \Omega_{ir}))^{m_{ir}}/2\mathrm{b}_{ir}$, $\beta_{ir} = 1/2\mathrm{b}_{ir}$, and $\delta_{ir} = \Omega_{ir}/(2\mathrm{b}_{ir})(2\mathrm{b}_{ir} m_{ir} + \Omega_{ir})$, Ω_{ir} and $2\mathrm{b}_{ir}$ are the respective average power of the LOS and multipath components, m_{ir} is the fading severity parameter, $\zeta(\kappa) = (-1)^{\kappa}(1-m_{ir})_{\kappa}\delta_{ir}^{\kappa}/(\kappa!)^2$, and $(\cdot)_{\kappa}$ denotes the Pochhammer symbol [21, p. xliii]. Here, m_{ir} represents the integer-valued fading severity parameter and ${}_1F_1(\cdot;\cdot;\cdot)$ denotes the confluent hypergeometric function of first kind [21]. Further, the free space loss factor $\mathcal{L}_{sr}$ corresponding to $S \to R$ link is given by [15] $\mathcal{L}_{sr} = \frac{1}{\mathcal{K}_{\mathcal{B}}\mathcal{T}\mathcal{W}}\left(\frac{c}{4\pi f_c w_{sr}}\right)^2$, where $\mathcal{K}_{\mathcal{B}} = 1.38 \times 10^{-23}$J/K is the Boltzman constant, $\mathcal{T}$ is the receiver noise temperature, $\mathcal{W}$ is the carrier bandwidth, c is the speed of light, f_c is the carrier frequency, and w_{ir} represent the distance as defined in the previous subsection. Also, the equivalent beam gain is $\vartheta_s \vartheta(\theta_{sr})$ corresponding to $S \to R$ link. Here, ϑ_s is the antenna gain of S, and the term $\vartheta(\theta_{sr})$ is given by $\vartheta(\theta_{sr}) = \vartheta_{sr}\left(\frac{\mathcal{J}_1(\rho_{sr})}{2\rho_{sr}} + 36\frac{\mathcal{J}_3(\rho_{sr})}{\rho_{sr}^3}\right)$, where θ_{sr} is the angular separation of R from the beam center of S, ϑ_{sr} is the antenna gain at node R, $\mathcal{J}_{\varrho}(\cdot)$, $\varrho \in \{1, 3\}$ is the Bessel function, and $\rho_{sr} = 2.07123\frac{\sin\theta_{sr}}{\sin\theta_{sr3\mathrm{dB}}}$ with $\theta_{sr3\mathrm{dB}}$ as 3dB beamwidth. Furthermore, the path loss for $H_j \to R$ link is given by $w_{h_j r}^{-\alpha}$ where α is the path loss exponent.

2) $R \to E$ and $U \to E$ links' channels: The channel coefficients g_{re} and g_{ue} for $R \to E$ and $U \to E$ links follow Rician and Nakagami-*m* fading, respectively. Thus, the pdf of the squared channel gain $|g_{re}|^2$ is given by

$$f_{|g_{re}|^2}(x) = \frac{(1+K_{re})}{\Omega_{re}} \exp\left(-K_{re} - \frac{(1+K_{re})x}{\Omega_{re}}\right) \times I_0\left(2\sqrt{\frac{K_{re}(1+K_{re})x}{\Omega_{re}}}\right), x \geq 0, \tag{2}$$

where K_{re} is the Rician factor, Ω_{re} is the average channel power, and $I_0(\cdot)$ denotes the modified Bessel function of zero order [21].

Further, the pdf of the channel gain $|g_{ue}|^2$ is given by

$$f_{|g_{ue}|^2}(x) = \left(\frac{m_{ue}}{\Omega_{ue}}\right)^{m_{ue}} \frac{x^{m_{ue}-1}}{\Gamma(m_{ue})} \exp\left(-\frac{m_{ue}}{\Omega_{ue}}x\right), \tag{3}$$

where m_{ue} and Ω_{ue} represent the fading severity parameter and average channel power, respectively.

C. Propagation Model

The satellite S in the first hop transmits its unit energy signal x_s towards the aerial relay R with power P_s. Hence, the signal received at R is given as

$$y_r = \sqrt{P_s \mathcal{L}_{sr} \vartheta_s \vartheta(\theta_{sr})} g_{sr} x_s + \sum_{j=1}^{M} \sqrt{P_j w_{h_j r}^{-\alpha}} g_{h_j r} x_j + n_r, \tag{4}$$

where P_j is the transmit power of jth HAP interferer, x_j is the unit energy signal of jth HAP interferer, and n_r is the AWGN. Using (4), we can represent the signal-to-interference-plus-noise ratio (SINR) at R as

$$\Lambda_{sr} = \frac{P_s \mathcal{L}_{sr} \vartheta_s \vartheta(\theta_{sr}) \left|g_{sr}\right|^2}{\sum_{j=1}^{M} P_j \left|g_{h_j r}\right|^2 w_{h_j r}^{-\alpha} + \sigma^2}. \tag{5}$$

Considering an interference-limited scenario where the interference power in (5) is sufficiently larger than the noise power, the resulting signal-to-interference ratio (SIR) can be expressed as

$$\Lambda_{sr} \approx \frac{\eta_s \left|g_{sr}\right|^2}{\sum_{j=1}^{M} P_j \left|g_{h_j r}\right|^2 w_{h_j r}^{-\alpha} (\triangleq \mathcal{I})}, \tag{6}$$

where $\eta_s = P_s \mathcal{L}_{sr} \vartheta_s \vartheta(\theta_{sr})$.

The aerial relay R tries to decode the message signal received by it in the first hop. If the decoding is successful, the DF relay R re-encodes and forwards the decoded unit energy message signal x_r towards ground UE E with power P_r, Hence, the signal received at E can be expressed as

$$y_e = \sqrt{P_r w_{re}^{-\alpha}} g_{re} x_r + \sqrt{P_u w_{ue}^{-\alpha}} g_{ue} x_u + n_e, \tag{7}$$

where P_u is the transmit power of single LAP interferer U, x_u is the unit energy signal of U, and n_e is the AWGN, and α as path loss exponent. As a result, we can express the SINR at E as

$$\Lambda_{re} = \frac{P_r \left|g_{re}\right|^2 w_{re}^{-\alpha}}{P_u \left|g_{ue}\right|^2 w_{ue}^{-\alpha} + \sigma^2}. \tag{8}$$

Similar to that in (6), under an interference-limited scenario, the SINR at E in (8) can be expressed as the following SIR

$$\Lambda_{re} \approx \frac{P_r \left|g_{re}\right|^2 w_{re}^{-\alpha}}{P_u \left|g_{ue}\right|^2 w_{ue}^{-\alpha}}. \tag{9}$$

In this work, we consider the SIRs as given by (6) and (9) for the OP analysis.

III. Outage Probability Analysis

In this section, we evaluate the e2e OP for the considered HSATN system model.

The e2e OP of the considered HSATN with DF relay R for certain predefined threshold γ_{th} can be calculated as

$$\begin{aligned}\mathcal{P}_{\text{out}}(\gamma_{\text{th}}) &= \Pr\left[\min(\Lambda_{sr}, \Lambda_{re}) < \gamma_{\text{th}}\right] \\ &= 1 - \Pr\left[\Lambda_{sr} > \gamma_{\text{th}}, \Lambda_{re} > \gamma_{\text{th}}\right] \\ &= 1 - (1 - \mathcal{P}_{\text{out}}^{sr}(\gamma_{\text{th}}))(1 - \mathcal{P}_{\text{out}}^{re}(\gamma_{\text{th}})),\end{aligned} \tag{10}$$

where $\mathcal{P}_{\text{out}}^{sr}(\gamma_{\text{th}})$ and $\mathcal{P}_{\text{out}}^{re}(\gamma_{\text{th}})$ represent the OP of $S-R$ and $R-E$ links, respectively. We first proceed to derive the OP term $\mathcal{P}_{\text{out}}^{sr}(\gamma_{\text{th}})$ based on the SIR as given in (6). Note that the mathematical derivation of $\mathcal{P}_{\text{out}}^{sr}(\gamma_{\text{th}})$ is quite challenging due to the involvement of multiple random variables corresponding to SR fading channel coefficients and HAP interferers' distances from R. We can calculate $\mathcal{P}_{\text{out}}^{sr}(\gamma_{\text{th}})$ as

$$\begin{aligned}\mathcal{P}_{\text{out}}^{sr}(\gamma_{\text{th}}) &= \Pr\left[\Lambda_{sr} < \gamma_{\text{th}}\right] \\ &= \Pr\left[\frac{\eta_s |g_{sr}|^2}{\sum_{j=1}^{M} P_j |g_{h_j r}|^2 w_{h_j r}^{-\alpha}} < \gamma_{\text{th}}\right] \\ &= \mathbb{E}_{\mathcal{I}}\left\{\Pr\left[|g_{sr}|^2 < \frac{\gamma_{\text{th}}\mathcal{I}}{\eta_s}\middle|\mathcal{I}\right]\right\} \\ &= \mathbb{E}_{\mathcal{I}}\left\{F_{|g_{sr}|^2}\left(\frac{\gamma_{\text{th}}\mathcal{I}}{\eta_s}\middle|\mathcal{I}\right)\right\},\end{aligned} \tag{11}$$

where $F_{|g_{sr}|^2}(\cdot|\mathcal{I})$ denotes the conditional cumulative distribution function (cdf) of random variable $|g_{sr}|^2$ conditioned on $\mathcal{I}$ and $\mathbb{E}_{\mathcal{I}}\{\cdot\}$ denotes the expectation with respect to $\mathcal{I}$. Hereby, the required cdf $F_{|g_{sr}|^2}(\cdot|\mathcal{I})$ can be calculated based on the SR pdf given in (1) which yields

$$\begin{aligned}F_{|g_{sr}|^2}\left(\frac{\gamma_{\text{th}}\mathcal{I}}{\eta_s}\middle|\mathcal{I}\right) &= 1 - \alpha_{sr} \sum_{k_1=0}^{m_{sr}-1} \xi(k) \\ &\times \sum_{p_1=0}^{k_1} \frac{k_1!}{p_1!} (\beta_{sr} - \delta_{sr})^{-(k_1+1-p_1)} \left(\frac{\gamma_{\text{th}}\mathcal{I}}{\eta_s}\right)^{p_1} \\ &\times \exp\left(-\frac{(\beta_{sr} - \delta_{sr})\gamma_{\text{th}}\mathcal{I}}{\eta_s}\right).\end{aligned} \tag{12}$$

Now, taking the expectation of (12) with respect to $\mathcal{I}$, we get

$$\begin{aligned}\mathcal{P}_{\text{out}}^{sr}(\gamma_{\text{th}}) = 1 - \alpha_{sr} \sum_{k_1=0}^{m_{sr}-1} \xi(k) \sum_{p_1=0}^{k_1} \frac{k_1!}{p_1!} (\beta_{sr} - \delta_{sr})^{-(k_1+1-p_1)} \\ \times \left(\frac{\gamma_{\text{th}}}{\eta_s}\right)^{p_1} \underbrace{\mathbb{E}_{\mathcal{I}}\left\{\mathcal{I}^{p_1} \exp\left(-\frac{(\beta_{sr} - \delta_{sr})\gamma_{\text{th}}\mathcal{I}}{\eta_s}\right)\right\}}_{\Psi}.\end{aligned} \tag{13}$$

The term Ψ in (13) can be calculated as

$$\Psi = (-1)^{p_1} \frac{\partial^{p_1} \mathbb{L}_{\mathcal{I}}(v)}{\partial v^{p_1}}\bigg|_{v=(\beta_{sr}-\delta_{sr})\gamma_{\text{th}}/\eta_s}, \tag{14}$$

where $\mathbb{L}_{\mathcal{I}}(v) = \mathbb{E}_{\mathcal{I}}\{\exp(-v\mathcal{I})\}$. Let us consider channels $g_{h_j r}$ to be i.i.d. for all j and redefine the SR distribution parameters $m_{h_j r}$, $\flat_{h_j r}$ and $\Omega_{h_j r}$ as m_{hr}, $\flat_{hr}$ and Ω_{hr}, respectively. Eventually, we define $\alpha_{h_j r} = \alpha_{hr}$, $\beta_{h_j r} = \beta_{hr}$, $\delta_{h_j r} = \delta_{hr}$, and $P_j = \eta_h$ for all j. We further consider the distance $w_{h_j r}$ as i.i.d. for all j. Hence, using the expression

of $\mathcal{I}$ in (14), we can write

$$\begin{aligned}\mathbb{L}_{\mathcal{I}}(v) &= \mathbb{E}_{\mathcal{I}}\left\{\exp\left(-v\sum_{j=1}^{M}\eta_h|g_{h_jr}|^2 w_{h_jr}^{-\alpha}\right)\right\}\\ &\overset{(a)}{=} \mathbb{E}_{w_{h_jr}}\mathbb{E}_{g_{h_jr}}\left\{\prod_{j=1}^{M}\left\{\exp\left(-v\eta_h|g_{h_jr}|^2 w_{h_jr}^{-\alpha}\right)\right\}\right\}\\ &= \mathbb{E}_{w_{h_jr}}\left\{\prod_{j=1}^{M}\int_0^{\infty}\exp\left(-v\eta_h x w_{h_jr}^{-\alpha}\right) f_{|g_{h_jr}|^2}(x)\,dx\right\}\\ &\overset{(b)}{=} \mathbb{E}_{w_{h_jr}}\Bigg\{\prod_{j=1}^{M}\alpha_{hr}\sum_{k_2=0}^{m_{hr}-1}\xi(k_2)\int_0^{\infty}x^{k_2}\\ &\qquad\times\exp\left(-x\left(v\eta_h w_{h_jr}^{-\alpha}+\beta_{hr}-\delta_{hr}\right)\right)dx\Bigg\}\\ &= \mathbb{E}_{w_{h_jr}}\Bigg\{\prod_{j=1}^{M}\alpha_{hr}\sum_{k_2=0}^{m_{hr}-1}\xi(k_2)\\ &\qquad\times\frac{k_2!}{(v\eta_h w_{h_jr}^{-\alpha}+\beta_{hr}-\delta_{hr})^{k_2+1}}\Bigg\}, \end{aligned}\tag{15}$$

where (a) follows the independence of w_{h_jr} and g_{h_jr}, and (b) follows the substitution of pdf $f_{|g_{h_jr}|^2}(\cdot)$. To perform the expectation with respect to w_{h_jr} in (15), we need to find the pdf of distance w_{h_jr}. For this purpose, we rely on the result given in [20] and introduce the following definitions: Let $R_E = 6371$ km as the radius of earth, the radial distances $OA = U_1 = 8371$ km and $OC = U_2 = 6531$ km, the apex angle subtended by the radial distances OA and OB at O as ϕ, and the distance between O and R as $w_r = w_{re}+R_E$. Furthermore, by adopting a spherical coordinate system, the location of H_j can be given as $(r_{h_j}, \theta_j, \psi_j)$, where $U_2 \le r_{h_j} \le U_1$, $0 \le \theta_j \le \phi/2$, $0 \le \psi \le 2\pi$. Hence, the required pdf of w_{h_jr} can be expressed as

$$f_{w_{h_jr}}(y) = \tau\left[\omega^2(y) - \rho^2(y)\right], \tag{16}$$

where $\omega(y) = \min\left(U_1, w_r+\sqrt{y}\right)$, $\rho(y) = \max\left(U_2, w_r\cos\frac{\phi}{2}+\sqrt{y-w_r^2\sin^2\frac{\phi}{2}}\right)$, and $\tau = \frac{3}{4w_r\left(1-\cos\frac{\phi}{2}\right)\left(U_1^3-U_2^3\right)}$. Now, applying the pdf given by (16) in (15) and thereby taking the expectation, we obtain

$$\begin{aligned}\mathbb{L}_{\mathcal{I}}(v) = \prod_{j=1}^{M}\alpha_{hr}\sum_{k_2=0}^{m_{hr}-1}\xi(k_2)\,k_2!\\ \times\int_{w_{\min}^2}^{w_{\max}^2}\frac{\tau\left[\omega^2(x)-\rho^2(x)\right]}{(v\eta_h x^{-\alpha}+\beta_{hr}-\delta_{hr})^{k_2+1}}dx,\end{aligned}\tag{17}$$

$w_{\min} = U_2 - w_r$ and $w_{\max} = \sqrt{U_1^2+w_r^2-2U_1 w_r\cos\frac{\phi}{2}}$. Finally, on solving (17) using Chebyshev-Gauss quadrature method and invoking the result into (13), we can calculate the OP of $S-R$ link, i.e., $\mathcal{P}_{\text{out}}^{sr}(\gamma_{\text{th}})$ as

$$\begin{aligned}\mathcal{P}_{\text{out}}^{sr}(\gamma_{\text{th}}) = 1-\alpha_{sr}\sum_{k_1=0}^{m_{sr}-1}\xi(k_1)\sum_{p_1=0}^{k_1}(-1)^{p_1}\frac{k_1!}{p_1!}\\ \times(\beta_{sr}-\delta_{sr})^{-(k_1+1-p_1)}\left(\frac{\gamma_{\text{th}}}{\eta_s}\right)^{p_1}\\ \times\left.\frac{\partial^{p_1}\mathbb{L}_{\mathcal{I}}(v)}{\partial v^{p_1}}\right|_{v=(\beta_{sr}-\delta_{sr})\gamma_{\text{th}}/\eta_s}.\end{aligned}\tag{18}$$

We next proceed to derive the OP term $\mathcal{P}_{\text{out}}^{re}(\gamma_{\text{th}})$ based on the SIR as given in (9). For a target threshold γ_{th}, we can calculate $\mathcal{P}_{\text{out}}^{re}(\gamma_{\text{th}})$ as

$$\begin{aligned}\mathcal{P}_{\text{out}}^{re}(\gamma_{\text{th}}) &= \Pr\left[\Lambda_{re} < \gamma_{\text{th}}\right]\\ &= \Pr\left[\frac{P_r|g_{re}|^2 w_{re}^{-\alpha}}{P_u|g_{ue}|^2 w_{ue}^{-\alpha}} \le \gamma_{\text{th}}\right]\\ &= \Pr\left[\frac{|g_{re}|^2}{|g_{ue}|^2} < \frac{P_u\gamma_{th}w_{re}^{\alpha}w_{ue}^{-\alpha}}{P_r}\right].\end{aligned}\tag{19}$$

To solve (19), we first define $X = |g_{re}|^2$ and $Y = |g_{ue}|^2$, and $Z = \frac{X}{Y}$. Then, we calculate the cdf of Z as

$$F_Z(z) = \Pr\left[Z \le z\right] = 1 - \mathbb{E}_X\left\{F_Y\left(\frac{x}{z}\middle|X\right)\right\}, \tag{20}$$

where $F_Y(\cdot|X)$ denotes the cdf of Y conditioned on X. Note that the cdf of Y can be calculated by using the pdf in (3) as $F_Y(y) = 1 - \frac{\Gamma\left(m_{ue}, \frac{m_{ue}y}{\Omega_{ue}}\right)}{\Gamma(m_{ue})}$, where $\Gamma(\cdot)$ denotes the upper incomplete gamma function. By using the cdf $F_Y(\cdot)$ and the pdf of X given by (2) in (20), and solving the resulting integral by applying the series form of $\Gamma(\cdot)$ followed by a change of variable operation, we obtain

$$\begin{aligned}F_Z(z) = \Upsilon_1\sum_{n=0}^{m_{ue}-1}\left(\frac{m_{ue}}{z}\right)^n\left(\Upsilon_2+\frac{m_{ue}}{z}\right)^{-(n+1)}\\ \times_1 F_1\left(n+1;1;\frac{\Upsilon_3^2}{\Upsilon_2+\frac{m_{ue}}{z}}\right),\end{aligned}\tag{21}$$

where $\Upsilon_1 = \frac{(1+K_{re})}{\Omega_{re}}\exp(-K_{re})$, $\Upsilon_2 = \frac{K_{re}(1+K_{re})}{\Omega_{re}}$ and $\Upsilon_3 = \sqrt{\frac{K_{re}(1+K_{re})}{\Omega_{re}}}$. Now, based on (21), the (19) can now be evaluated as

$$\begin{aligned}\mathcal{P}_{\text{out}}^{re}(\gamma_{\text{th}}) &= \mathbb{E}_{w_{ue}}\left\{F_Z\left(\frac{P_u\gamma_{\text{th}}w_{re}^{\alpha}w_{ue}^{-\alpha}}{P_r}\middle|w_{ue}\right)\right\}\\ &= \Upsilon_1\sum_{n=0}^{m_{ue}-1}\left(\frac{m_{ue}P_r}{P_u\gamma_{\text{th}}w_{re}^{\alpha}}\right)^n\\ &\times\int_0^{\infty}x^{-n\alpha}\left(\Upsilon_2+\frac{m_{ue}P_r}{P_u\gamma_{\text{th}}x^{-\alpha}w_{re}^{\alpha}}\right)^{-(n+1)}\\ &\times_1 F_1\left(n+1;1;\frac{\Upsilon_3^2}{\Upsilon_2+\frac{m_{ue}P_R}{P_U\gamma_{\text{th}}w_{re}^{\alpha}x^{-\alpha}}}\right)f_{w_{ue}}(x)dx.\end{aligned}\tag{22}$$

To solve (22), the required pdf of random distance w_{ue} can be found in [5] as

$$f_{w_{ue}}(x) = \frac{2x}{L^2}, w_{re} \le x \le \sqrt{w_{re}^2+L^2}. \tag{23}$$

Finally, using (23) in (22), we obtain the OP of $R-E$ link, i.e., $\mathcal{P}_{\text{out}}^{re}(\gamma_{\text{th}})$ as

$$\mathcal{P}_{\text{out}}^{re}(\gamma_{\text{th}}) = \Upsilon_1 \sum_{n=0}^{m_{ue}-1} \left(\frac{m_{ue}P_r}{P_u\gamma_{\text{th}}w_{re}^{\alpha}}\right)^n \times \int_{w_{re}}^{\sqrt{w_{re}^2+L^2}} x^{n\alpha}\left(\Upsilon_2 + \frac{m_{ue}P_r}{P_u\gamma_{\text{th}}x^{-\alpha}w_{re}^{\alpha}}\right)^{-(n+1)} \times_1 F_1\left(n+1;1;\frac{\Upsilon_3^2}{\Upsilon_2+\frac{m_{ue}P_r}{P_u\gamma_{\text{th}}w_{re}^{\alpha}x^{-\alpha}}}\right)\frac{2x}{L^2}dx. \quad (24)$$

Based on (18) and (24), the e2e OP in (10) can be evaluated.

IV. Numerical Results

In this section, we provide numerical results to study the performance of considered HSATN system model. We set satellite link parameters as $\mathcal{T} = 300$ K, $\mathcal{W} = 15$ MHz, c = 3×10^8 m/s, $w_{sr} = 35,781$ Km, $f_{\text{c}} = 2$ GHz, $\vartheta_s = 53.45$ dB, $\vartheta_r = 4.8$ dB, $\theta_{sr} = 0.8°$. We further set the SR fading parameters $(m_{ir}, \flat_{ir}, \Omega_{ir}) = (2, 10 \text{ dB}, 2 \text{ dB})$ where $i \in \{s, h\}$. The path loss factor α for $R \to E$ link is set as 2 along with the parameters $(m_{ue}, \Omega_{ue}) = (2, 1 \text{ dB})$. We set the threshold value as $\gamma_{\text{th}} = 0$ dB. Simulations are also performed to validate the theoretical analysis.

Fig. 2 plots the OP of $S \to R$ link against η_s for various values of U_2, M and ϕ. Here, we fix $L = 10$ km and $w_{re} = 5$ km. From the OP curves for $(M, \phi) = (4, \pi/3)$ and $(4, \pi/6)$, we observe that the OP of the system becomes poor when ϕ increases for given values of M and U_2. Similar observations can be made from the curves for different values of U_2 for given values of M and ϕ. Here, the HAPs' deployment region expands when either ϕ or U_2 takes on a larger value resulting in an increased path loss. Further, the curves for $(M, \phi) = (1, \pi/3)$ and $(4, \pi/3)$ reveal that the OP of the system deteriorates when M increases for given values of ϕ and U_2. It follows from the fact that increasing the value of M results in more interference at the node R.

Fig. 3 plots the OP of $R \to E$ link against P_r for various values of P_u and w_{re} with fixed L. Here, we set the parameters $(K_{re}, \Omega_{re}) = (1, 1 \text{ dB})$ and $L = 20$ km. We consider $P_u = 20$ dB and $P_u = 10$ dB to plot the OP curves for three values of w_{re}, i.e., 5 km, 15 km, and 30 km. We found that the OP of the system decreases when w_{re} decreases for a given value of P_u. This stems from the fact that a higher value of w_{re} corresponds to an increased path loss which causes reduction in the received SNR at E. However, when P_u takes on a higher value, the OP of the system detereorates due to increased interference power.

Fig. 4 plots the e2e OP of the considered system against η_s for various values of M, w_{re} and ϕ. Here, we fix $L = 10$ km. We observe that for given values of w_{re} and ϕ, the e2e OP deteriorates with increase of M. Further, we observe that for fixed values of w_{re} and M, the e2e OP degrades when ϕ increases. We can also see that simulations verify the theoretical results.

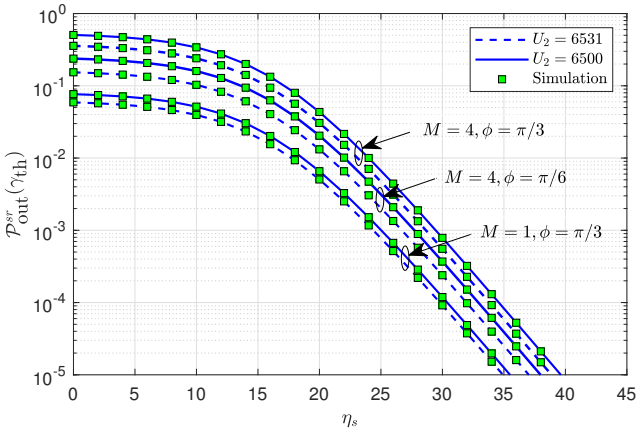

Fig. 2. OP of $S \to R$ link versus η_s for variable U_2, M and ϕ.

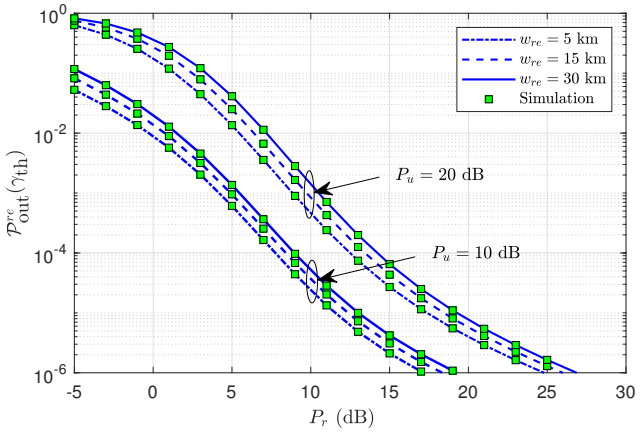

Fig. 3. OP of $R \to E$ link versus P_r for variable w_{re} and P_u.

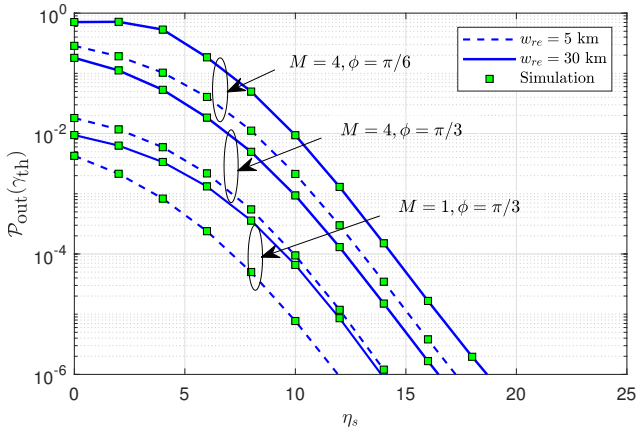

Fig. 4. End-to-end OP versus η_s for variable w_{re}, M and ϕ.

V. Conclusion

This paper has evaluated the outage performance of an HSATN where a DF-based aerial relay aides the commu-

nication from a satellite to ground UE in the presence of interference. Specifically, the multiple HAPs uniformly located in a 3D spherical sector above the surface of earth were assumed to cause interference at aerial relay in the first hop. Further, a single LAP interferer deployed in a cylindrical terrestrial small cell was assumed to cause interference at ground UE. For this set-up, the OP expressions for first and second hops along with the e2e communication were derived. We depicted the impact of the distance between aerial relay and ground UE on the OP of considered HSATN.

VI. Acknowledgement

This work was supported by the Science and Engineering Research Board, Department of Science and Technology, Govt. of India (Project no. SRG/2019/000979).

References

[1] G. Giambene, S. Kota, and P. Pillai, "Satellite-5G integration: A network perspective," *IEEE Netw.*, vol. 32, no. 5, pp. 25-31, Sep./Oct. 2018.

[2] A. Guidotti et al., "Architectures and key technical challenges for 5G systems incorporating satellites," *IEEE Trans. Veh. Technol.*, vol. 68, no. 3, pp. 2624-2639, Mar. 2019.

[3] B. Evans, M. Werner, E. Lutz, M. Bousquet, G. Corazza, G. Maral, and R. Rumeau, "Integration of satellite and terrestrial systems in future media communications," *IEEE Wireless Commun.*, vol. 12, no. 5, pp. 72-80, Oct. 2005.

[4] S. Sreng, B. Escrig, M.-L. Boucheret, "Exact symbol error probability of hybrid/integrated satellite-terrestrial cooperative network," *IEEE Trans. Wireless Commun.,* vol. 12, no. 3, pp. 1310-1319, Mar. 2013.

[5] V. V. Chetlur and H. S. Dhillon "Downlink coverage analysis for a finite 3-D wireless network of unmanned aerial vehicles," *IEEE Trans. Commun.*,vol. 65, no. 10, pp. 4543-4557, Oct.2017.

[6] S. Hu, J. Flordelis, F. Rusek, and O. Edfors "Unmanned aerial vehicle assisted cellular communication," *ArXiv Preprint*, arXiv: 1803.05763, 2018.

[7] P. K. Sharma and D. I. Kim, "Random 3D mobile UAV networks: Mobility modeling and coverage probability," *IEEE Trans. Wireless Commun.*, vol. 18, no. 5, pp. 2527-2538, May 2019.

[8] B. Li, Z. Fei, and Y. Zhang, "UAV communications for 5G and beyond: Recent advances and future trends," *ArXiv Preprint*, arXiv: 1901.06637, 2019.

[9] M. R. Bhatnagar and Arti M. K., "Performance analysis of AF based hybrid satellite-terrestrial cooperative network over generalized fading channels," *IEEE Commun. Lett.*, vol. 17, no. 10, pp. 1912-1915, Oct. 2013.

[10] P. K. Upadhyay and P. K. Sharma, "Max-max user-relay selection scheme in multiuser and multirelay hybrid satellite-terrestrial relay systems," *IEEE Commun. Lett.*, vol. 20, no. 2, pp. 268-271, Feb. 2016.

[11] P. K. Sharma, P. K. Upadhyay, D. B. da Costa, P. S. Bithas, and A. G. Kanatas, "Performance analysis of overlay spectrum sharing in hybrid satellite-terrestrial systems with secondary network selection," *IEEE Trans. Wireless Commun.*, vol. 16, no. 10, pp. 6586-6601, Oct. 2017.

[12] K. An, M. Lin, T. Liang, J. Wang, J. Wang, Y. Huang, and A. L. Swindlehurst, "Performance analysis of multi-antenna hybrid satellite-terrestrial relay networks in the presence of interference," *IEEE Trans. Commun.*, vol. 63, no. 11, pp. 4390–4404, Nov. 2015.

[13] L. Yang and M. O. Hasna, "Performance analysis of amplify-and-forward hybrid satellite-terrestrial networks with cochannel interference," *IEEE Trans. Commun.*, vol. 63, no. 12, pp. 5052–5061, Dec. 2015.

[14] K. Guo, M. Lin, B. Zhang, W. Zhu, J. Wang, and T. A. Tsiftsis, "On the performance of LMS communication with hardware impairments and interference," *IEEE Trans. Commun.*, vol. 67, no. 2, pp. 1490–1505, Feb. 2019.

[15] P. K. Sharma, B. Yogesh, D. Gupta, and D. I. Kim, "Performance analysis of IoT-based overlay satellite-terrestrial networks under the interference," *IEEE Trans. on Cogn. Commun. Netw.*, vol. 7, no. 3, pp. 985-1001, Sept. 2021.

[16] Y. Zeng, R. Zhang, and T. J. Lim "Throughput maximization for UAV-enabled mobile relaying systems," *IEEE Trans. Commun.*, vol. 64, no. 12, pp. 4983-4996, Dec. 2016.

[17] L. Yang, J. Chen, M. O. Hasna, and H. -C. Yang, "Outage performance of UAV-assisted relaying systems with RF energy harvesting," *IEEE Commun. Lett.*, vol. 22, no. 12, pp. 2471-2474, Dec. 2018.

[18] P. K. Sharma, D. Deepthi, and D. I. Kim, "Outage probability of 3-D mobile UAV relaying for hybrid satellite-terrestrial networks," *IEEE Commun. Lett.*, vol. 24, no. 2, pp. 418-422, Feb. 2020.

[19] P. K. Sharma and D. I. Kim, "Secure 3D mobile UAV relaying for hybrid satellite-terrestrial networks," *IEEE Trans. Wireless Commun.*, vol. 19, no. 4, pp. 2770-2784, Apr. 2020.

[20] G. Pan, J. Ye, Y. Zhang, and M. -S. Alouini, "Performance analysis and optimization of cooperative satellite-aerial-terrestrial systems," *ArXiv Preprint*, arXiv:2006.11854, 2020.

[21] I. S. Gradshteyn and I. M. Ryzhik, *Tables of Integrals, Series and Products*, 6th ed. New York: Academic Press, 2000.